

## Fine-structure in $3d^4$ States of Highly Charged Ti-like Ions

Daiji Kato<sup>a\*</sup> (加藤太治), Xiao-Min Tong<sup>a</sup> (仝曉民), Hirofumi Watanabe<sup>a</sup> (渡邊裕文),  
Tsunemitsu Fukami<sup>b</sup> (深見恒光), Tohru Kinugawa<sup>a</sup> (絹川亨), Chikashi Yamada<sup>a,b</sup> (山田千樞),  
Shunsuke Ohtani<sup>a,b</sup> (大谷俊介) and Tsutomu Watanabe<sup>c†</sup> (渡部力)  
<sup>a</sup>Cold Trapped Ions Project, ICORP, JST, 1-40-2 Tokyo 182-0024, Japan  
<sup>b</sup>University of Electro-Communications, Tokyo 182-8585, Japan  
<sup>c</sup>International Christian University, Tokyo 181-8585, Japan

A remarkable improvement of *ab initio* calculations was obtained for wave lengths of ( $3d^4$ )  $J = 3 \rightarrow 2$  forbidden transition. Present calculations reduced the long-standing discrepancy from measurements down to less than 0.2% for most high- $Z$  titanium-like ions. In the present calculations, a large extent of configuration space was included so that most important many-body effects were taken into account. To this end, the linearized second-order Brillouin-Wigner perturbation theory was employed with optimized spin-orbitals. Transition probability and atomic  $g$ -factor were also calculated with the improved atomic wavefunctions.

### INTRODUCTION

From a survey of atomic transitions using the multi-configuration Dirac-Fock (MCDF) method, Feldman, Indelicato and Sugar<sup>1</sup> reported that a forbidden transition between the lowest fine-structure levels of ( $3d^4$ )  $J = 2$  and  $J = 3$  was to be observed in the optical region for most high- $Z$  titanium-like ions. Besides its potential importance for high-temperature plasma diagnostics, the transition serves as a test-ground for many-body atomic structure theories, as will be seen shortly.

The first observation of the transition was made by Morgan et al.<sup>2</sup> for  $Xe^{32+}$  and  $Ba^{34+}$ . However, measured wavelengths were found to have an unexpectedly large discrepancy ( $\cong 5\%$ ) from state-of-the-art MCDF calculations.<sup>3</sup> Indelicato<sup>4</sup> tried to refine the MCDF calculations by including some valence-core correlations, but eventually found little improvement due to almost complete cancellation. A typical energy difference of this transition is of  $10^{-5}$  relative to the individual energies. It suggests that a large extent of configuration space may participate in contributions to the wavelength. Beck<sup>5</sup> thoroughly investigated many sorts of the contributions by configuration interaction (CI) calculations, and reduced the discrepancy to  $\cong 1\%$ .

After the first measurement by Morgan et al.,<sup>2</sup> further wavelength measurements have been pursued by several groups.<sup>6-11</sup> Available measurements now cover a wide range of  $Z (= 51-83)$ . It is noteworthy that, in Ref. 10, wave lengths for unmeasured elements in  $Z = 52-83$  were evaluated by in-

terpolating and extrapolating some available measurements; uncertainties in the evaluations were estimated to be within 0.1% that were much smaller than errors of the improved calculations by Beck.<sup>5</sup> The set of measurements thus serves as a benchmark for improvements of the many-body atomic structure theories.

In this paper, an efficient *ab initio* theoretical method is devised for further improvement of the calculations. With the devised method, calculations of the transition wavelength, the magnetic-dipole transition probability and the atomic  $g$ -factor are presented for the lowest fine-structure levels in the  $3d^4$  state.

### THEORETICAL METHOD

As already mentioned, a large extent of configuration space is involved in the transition, though the bulk of the configuration space has only marginal contributions to individual atomic states. In such a case, it is useless to perform all-order many-body calculations with the whole configuration space. A natural remedy to the useless computational burden is to adopt the perturbation theory to the marginal part of the configuration space.

The whole configuration space is divided into a principal part ( $P$ ) and an orthogonal complementary part ( $Q$ ). Interaction between  $P$  and  $Q$  is assumed to be the lowest-order perturbation. Total energy functional is partitioned into the

\* Corresponding author. E-mail: kato@hci.jst.go.jp, Phone: +81-424-83-1094, Fax: +81-424-83-1409

† Present address: Institute for Laser Science, University of Electro-Communications, Tokyo 182-8585, Japan  
Special issue for the Fourth Asian International Seminars on Atomic and Molecular Physics

zero-order part ( $H^{(0)}$ ) and the residual part ( $V$ ). The Dirac-Fock energy functional is chosen as the zero-order part; the residual part then represents a correlation energy functional. The second-order Brillouin-Wigner perturbation theory then leads to,

$$\begin{aligned} (E - H_{QQ}^{(0)})^{-1} V_{QP} \Psi_P &= \Psi_Q, \\ [H_{PP}^{(0)} + V_{PP} + V_{PQ}(E - H_{QQ}^{(0)})^{-1} V_{QP}] \Psi_P &= E \Psi_P. \end{aligned} \quad (1)$$

The above equations define the first-order correlation operator and the second-order effective Hamiltonian operator for the  $P$ -space, respectively. In the brackets of the second equation, the first and second terms compose the total energy functional in the  $P$ -space, and the third term represents the second-order correction to the correlation energy functional in the  $P$ -space. The non-linear effective Hamiltonian equation is written in a linearized form,

$$\begin{pmatrix} H_{PP}^{(0)} + V_{PP} & V_{PQ} \\ V_{QP} & H_{QQ}^{(0)} \end{pmatrix} \begin{pmatrix} \Psi_P \\ \Psi_Q \end{pmatrix} = E \begin{pmatrix} \Psi_P \\ \Psi_Q \end{pmatrix}. \quad (2)$$

The requirement that the total energy functional ( $E$ ) is stationary with respect to variations in spin-orbitals ( $\{\phi\}$ ) under the normalization and the orthogonality conditions leads to a set of the Euler-Lagrange equations,

$$\frac{\delta E[\{\phi\}]}{\delta \phi_a} = \mu_a \phi_a + \sum_{b \neq a} \mu_{ab} \phi_b, \quad (3)$$

where  $\{\mu\}$  are the Lagrange multipliers. The above equations are nothing but reduced MCDF equations. That is to say, an apparent connection between the second-order Brillouin-Wigner perturbation energy functional and a set of the reduced MCDF equations is provided.

In the Hamiltonian matrix [Eq. 2],  $H_{QQ}^{(0)}$  block is diagonal. As a result, a computation time and file system size required for calculations of the matrix elements are reduced remarkably. The present method thus has the potential ability to

take a very large extent of the configuration space into account, which is almost inaccessible by full MCDF and CI methods, accurately with relatively small computational resources provided the  $Q$ -space contributes perturbatively to the  $P$ -space. Additionally, the present method is expected to be more effective than conventional perturbation theories, since spin-orbitals are optimized automatically to a given perturbation energy functional so that a total energy is stationary.

In the present calculations, the  $P$ -space was spanned by  $|0\rangle \equiv 1s^2 2s^2 2p^6 3s^2 3p^6 3d^4$ , and internal single and double excitations, i.e. in the second quantization formalism,  $a^\dagger_{3d} a_{3s} |0\rangle$ ,  $a^\dagger_{3d} a^\dagger_{3d} a_{3s} a_{3s} |0\rangle$  and  $a^\dagger_{3d} a^\dagger_{3d} a_{3p} a_{3p} |0\rangle$ . The three-, four-, fold excitations were omitted. Representative configurations in the  $Q$ -space were  $a^\dagger_{3d} a_{3l} |0\rangle$  ( $n = 4-7$ ) and  $a^\dagger_{3d} a^\dagger_{3d} a_{3l} a_{3l} |0\rangle$  ( $n = 4-6$ ), so that the core polarization and the valence correlation except for the valence-core correlation were included. It is noted that, in the above, the non-relativistic notation is used for simplicity. In Table 1, number of the spin-orbital configurations and partition of the whole configuration space are summarized. The lowest-order quantum electrodynamics corrections: the single transverse-photon exchange interaction and vacuum polarization, were included except for the self-energy correction. The nuclear charge distribution was represented by the spherical symmetric Fermi-model. The present calculations were implemented with the GRASP92 code.<sup>12</sup>

## RESULTS AND DISCUSSION

In Table 2, calculated wavelengths for the  $J = 3 \rightarrow 2$  forbidden transition are compared with the available measurements and the CI calculations by Beck.<sup>5</sup> The present agreement with the measurements is excellent; the discrepancy is less than 0.2% except for  $\text{Sb}^{29+}$  ( $\cong 0.5\%$  error) and  $\text{Xe}^{32+}$  ( $\cong 0.4\%$  error). For  $\text{Sm}^{40+}$  and  $\text{Eu}^{41+}$ , Watanabe et al.<sup>11</sup> observed

Table 1.

State	$J = 0$	$J = 1$	$J = 2$	$J = 3$	$J = 4$
$P$ -space					
$ 0\rangle$	5	4	8	6	7
$a^\dagger_{3d} a_{3s}  0\rangle$	4	11	17	17	12
$a^\dagger_{3d} a^\dagger_{3d} a_{3s} a_{3s}  0\rangle$	5	4	8	6	7
$a^\dagger_{3d} a^\dagger_{3d} a_{3p} a_{3p}  0\rangle$	30	61	94	87	79
$Q$ -space					
$a^\dagger_{3d} a_{3l}  0\rangle$	885	2470	3585	4074	3959
$a^\dagger_{3d} a^\dagger_{3d} a_{3l} a_{3l}  0\rangle$	1004	2607	3944	4428	4454

Number of the spin-orbital configurations and partition of configuration space. A vacuum state is formed from occupied orbitals:  $|0\rangle \equiv 1s^2 2s^2 2p^6 3s^2 3p^6 3d^4$ .  $v$  and  $w$  represent virtual orbitals of  $n = 4-7$  for the single excitation and of  $n = 4-6$  for the double excitation.

Table 2.

Z	Present calculation	Beck <sup>5</sup>	Measurements
51 (Sb <sup>29+</sup> )	472.905	-	470.24(3) <sup>11</sup>
53 (I <sup>31+</sup> )	430.705	-	430.33(8) <sup>11</sup>
54 (Xe <sup>32+</sup> )	415.644	407.93	413.88(7) <sup>11</sup> , 413.94(20) <sup>2</sup>
55 (Cs <sup>33+</sup> )	402.846	-	402.14(12) <sup>11</sup>
56 (Ba <sup>34+</sup> )	393.649	386.63	393.08(18) <sup>11</sup> , 393.24(20) <sup>2</sup> , 93.239(8) <sup>7</sup>
60 (Nd <sup>38+</sup> )	375.382	367.93	375.3(2) <sup>6</sup>
62 (Sm <sup>40+</sup> )	372.386	-	372.52(2) <sup>11</sup>
63 (Eu <sup>41+</sup> )	371.743	-	371.75(3) <sup>11</sup>
64 (Gd <sup>42+</sup> )	371.202	367.53	371.3(2) <sup>6</sup>
70 (Yb <sup>48+</sup> )	367.670	-	367.64(15) <sup>10</sup>
72 (Hf <sup>50+</sup> )	365.434	-	365.54(4) <sup>11</sup>
73 (Ta <sup>51+</sup> )	364.077	-	364.18(5) <sup>11</sup>
74 (W <sup>52+</sup> )	362.568	360.15	362.67(2) <sup>11</sup> , 362.713(10) <sup>9</sup> , 362.6(2) <sup>10</sup>
75 (Re <sup>53+</sup> )	360.917	-	361.06(5) <sup>11</sup>
78 (Pt <sup>56+</sup> )	355.211	-	355.44(4) <sup>11</sup>
79 (Au <sup>57+</sup> )	353.097	-	353.2(2) <sup>8</sup>
83 (Bi <sup>61+</sup> )	343.870	344.16	344.29(15) <sup>10</sup>

Wavelengths (nm) of  $(3d^4) J = 3 \rightarrow 2$  forbidden transition. Numbers in parentheses are experimental uncertainties, e.g. 393.08(18) represents  $393.08 \pm 0.18$ .

another forbidden transition of  $J = 3 \rightarrow 4$  with wave lengths of 369.89(3) nm and 339.48(4) nm, respectively. Present calculations are 371.20 nm and 340.94 nm, respectively, within 0.4% error. The valence-core correlation was examined for Nd<sup>38+</sup>, since it was omitted in the present calculations. It turned out to be as significant in the individual energies as the core polarization and the valence correlation. Nevertheless, it has little contribution to the wave length due to almost complete cancellation in the energy difference.

The present calculations and the measurements are

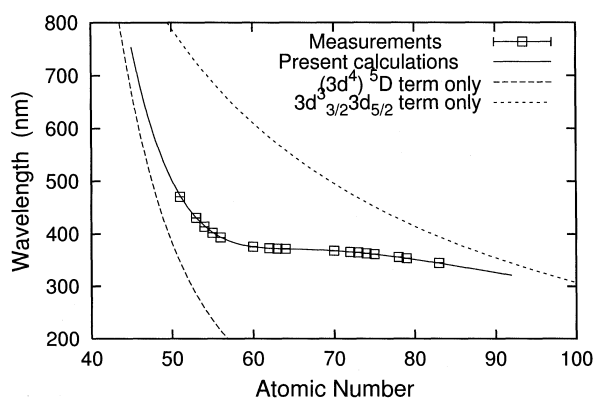


Fig. 1. Plateau in the wavelength change. Solid curve is plot of the present calculations, long-dash curve plot of calculations with  $(3d^4) {}^5D$  term only, short-dash curve plot of calculations with  $3d^3 3d_{5/2}$  term only, and open-squares measurements.

plot ted in Fig. 1. An intriguing feature seen is a plateau of wave length change in  $Z = 60-70$ . Such a fine-structure has been explored theoretically in other cases,<sup>4</sup> and the transitions with wave lengths almost independent on  $Z$  were found in the near infrared region for highly charged zirconium-like ( $4d^4$ ) and neodymium-like ( $4f^6$ ) ions too. Wave lengths for this sort of transition are expected to scale as  $Z^4$ , provided the transitions are in a single  $LS$ -term. In Ref. 13, however, it was pointed out that the  $LS$ -coupling scheme already failed in the  $Z$  range where the plateau took place. It suggests that in intermediate coupling in the  $3d^4$  state plays a crucial role in a mechanism by which the plateau takes place. To see this, wavelengths obtained from calculations with  $(3d^4) {}^5D$  term only and those with  $3d^3 3d_{5/2}$  term only are plotted in the figure. As expected, the wavelength for the  $(3d^4) {}^5D$  term falls rapidly into the shorter wavelength region as  $Z$  increases. On the contrary, it turns out that the wavelength for the  $3d^3 3d_{5/2}$  term decreases with so a gentle slope that the wavelength is found still in the optical region up to  $Z \cong 90$ . The realistic wavelength decreases rapidly along the former wavelength-curve in low- $Z$  region, and finds its way eventually to the latter wavelength-curve in high- $Z$  region. In the course, the plateau takes place in dictating the intermediate coupling switches from the  $LS$ -coupling to the  $jj$ -coupling in a rather narrow  $Z$  range.

In Fig. 2, the magnetic-dipole probabilities of the  $J = 3 \rightarrow 2$  and the  $J = 3 \rightarrow 4$  ( $J = 4 \rightarrow 3$  for  $Z < 52$ ) transitions are presented. Variation of the probabilities are not monotonic. A

vanishing probability of the  $J = 3 \rightarrow 4$  transition near  $Z = 52$  is due to a level crossing between  $J = 3, 4$ . The early MCDF calculations by Feldman et al.<sup>1</sup> are also plotted in the figure. The present calculations have smaller probabilities for both the transitions which is attributed probably to smaller energy differences of the present calculations; improvement always reduces the energy differences in the present case. The discrepancy disappears apparently in high- $Z$  region for the  $J = 3 \rightarrow 2$  transition. One and only one available measurement for  $\text{Xe}^{32+}$  by Serpa et al.<sup>14</sup> is also plotted in the figure. The discrepancy from the measurement amounts about 10%. It is noted that the electric-quadrupole contribution to this transition was calculated to be six orders of magnitude smaller than the magnetic-dipole. For the transition probabilities, there is no reason to cancel the individual contributions. The large discrepancy might be attributed to omission of the valence-core correlation in the present calculations.

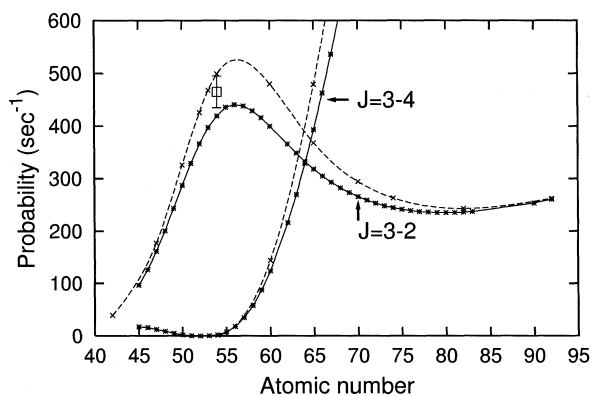


Fig. 2. Magnetic-dipole probabilities ( $\text{sec}^{-1}$ ) of  $J = 3 \rightarrow 2$  and  $J = 3 \rightarrow 4$  ( $J = 4 \rightarrow 3$  for  $Z < 52$ ) transitions. Solid curves are plot of the present calculations, dash curves plot of the MCDF calculations by Feldman et al.,<sup>1</sup> and a open-square the measurement by Serpa et al.<sup>14</sup> for  $\text{Xe}^{32+}$ .

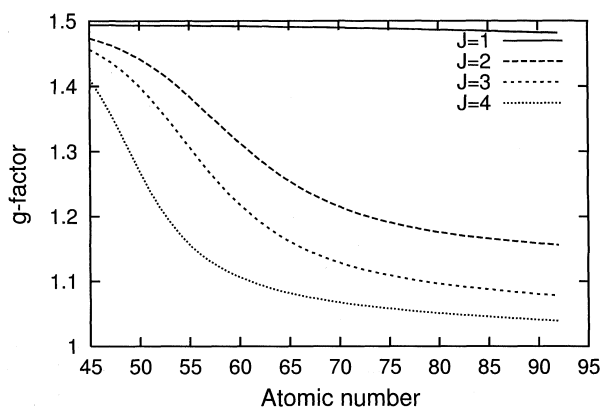


Fig. 3. Atomic  $g$ -factor for  $(3d^4) J = 1-4$ .

In Fig. 3, calculations of the atomic  $g$ -factor are shown for the lowest levels of  $(3d^4) J = 1-4$ . They decrease from the Landé's value (1.5 for  $^5D$  term) as  $Z$  increases. The  $g$ -factors of  $J = 2-4$  change by  $\sim 20\%$  in  $Z = 45-92$ , while the  $g$ -factor of  $J = 1$  changes little in the  $Z$  range. With the present  $g$ -factors, splitting in the Zeeman-induced triplet structure ( $\pi$ - and  $\sigma^{\pm}$ -components) of the  $J = 3 \rightarrow 2$  line was estimated to be  $\cong 1.9 \times 10^{-4}$  eV for  $\text{U}^{70+}$  at magnetic-field strength of 3 T, while to be  $\cong 2.6 \times 10^{-4}$  eV with the Landé's value. It indicates that such a high resolving power as  $>10^4$  is necessary to observe the triplet structure. Finer splitting within each component (the Zeeman shift) is even smaller:  $\cong 1.4 \times 10^{-5}$  eV for  $\text{U}^{70+}$ . A preliminary Fabry-Perot interferometry study<sup>15</sup> has been made for  $\text{Ba}^{34+}$ , but could not resolve the triplet structure due to the Doppler-broadening of the line.

In concluding remarks, an effective second-order perturbation theory was devised. The theory treats the principal configuration space up to all-order, while contribution of the complementary space is treated as the second-order perturbation. It reduces the computational time and the file system size remarkably, since the off-diagonal part of effective Hamiltonian matrix elements in the large complementary space can be omitted in the second-order calculations. An advantage over the conventional perturbation theory is that the spin-orbitals are optimized automatically to the perturbation energy functional by solving reduced MCDF type equations. The present calculations of the wavelength for transition between the lowest levels of  $(3d^4) J = 2$  and  $J = 3$  reduced the error in other theories down to less than 0.2% for most high- $Z$  elements. However, it might be too optimistic to be confident with the present calculations, since a choice of the principal configuration space is still somewhat an art. Convergence must be examined with respect to partitioning of the principal space as well as the size of the whole configuration space.

Received December 31, 2000.

### Key Words

*Ab initio* many-body atomic structure theory;  
Highly charged ions; Optical and forbidden transition.

### REFERENCES

- Feldman, U.; Indelicato, P.; Sugar, J. *J. Opt. Soc. Am.* **1991**, *B8*, 3.
- Morgan, C. A. et al. *Phys. Rev. Lett.* **1995**, *74*, 1716.

3. Kim, Y.-K. *Phys. Scr.* **1993**, T47, 54.
4. Indelicato, P. *Phys. Scr.* **1996**, T65, 57.
5. Beck, D. R. *Phys. Rev.* **1997**, A56, 2428; *Phys. Rev.* **1999**, A60, 3304.
6. Serpa, F. G. et al. *Phys. Rev.* **1996**, A53, 2220.
7. Bieber, D. J. et al. *Phys. Scr.* **1997**, T73, 64.
8. Trabert, E. et al. *Phys. Scr.* **1998**, 58, 599.
9. Utter, S. B.; Beiersdorfer, P.; Brown, G. V. *Phys. Rev.* **2000**, A61, 030503(R); Utter, S. B. et al. to be published in *Proceedings of the 10<sup>th</sup> International Conference on the Physics of Highly Charged Ions*, Berkeley, 2000.
10. Porto, J. V.; Kink, I.; Gillaspy, J. D. *Phys. Rev.* **2000**, A61, 054501.
11. Watanabe, H. et al. *Phys. Rev.* **2001**, A62, 042513.
12. Parpia, F. A.; Fischer, C. F.; Grant, I. P. *Comput. Phys. Commun.* **1996**, 94, 249.
13. Kato, D. et al. *Phys. Scr.* **1999**, T80, 446.
14. Serpa, F. G. et al. *Phys. Rev.* **1997**, A55, 4196.
15. Adler, H. et al. *Nuclear Instruments and Methods in Physics Research* **1995**, B98, 581.